RSC Advances

ROYAL SOCIETY OF CHEMISTRY

www.rsc.org/advances

RSC Advances

RSCPublishing

PAPER

Cite this: DOI: 10.1039/x0xx00000x

Surface PEGylation on PLA membranes via micro-swelling and crosslinking for improved biocompatibility/hemocompatibility

Received 00th January 2012,
Accepted 00th January 2012

DOI: 10.1039/x0xx00000x

www.rsc.org/

Xuemin Yu, Zhu Xiong, Jinglong Li, Ziyang Wu, Yunze Wang, Fu Liu*,

Poly (lactic acid) (PLA) has attracted growing attention as a sustainable and environmentally benign membrane material. The good biocompatibility/hemocompatibility is essential for hemodialysis membranes. To circumvent the inadequate hydrophilicity/biocompatibility/hemocompatibility, we have developed a feasible strategy that enables the persistent PEGylation on PLA membrane via micro-swelling and subsequent UV-initiated crosslinking of poly (ethylene glycol) diacrylate (PEGDA). The content of DMSO and PEGDA in the reaction solution was crucial to control the surface PEGylation in kinetics. Besides, the influence of PEGylation on membrane chemistry, morphology, hydrophilicity, water flux and dynamic fouling resistance to BSA was investigated. It was demonstrated that the biocompatibility/hemocompatibility was significantly improved by the surface PEGylation in aspect of reduced BSA adsorption, extended APTT and alleviative platelet adhesion.

Introduction

Hemodialysis membranes have been widely used for end stage renal disease (ESRD) patients. However, for most of current clinical dialysis membranes e.g. PS, PES or CA, none of which can satisfy the expectation of both doctors and patients. For example, the hydrophobic PES or PS membrane is prone to protein adsorption and platelet adhesion, resulting in the formation of thrombus, which is harmful and even lethal to the patients. Therefore, the anticoagulant e.g. heparin is necessary to be injected to prevent blood coagulation during hemodialysis. However, the large amount of heparin injection will lead to bleeding risk. In order to improve the blood compatibility of current membranes, tremendous repairing work including additive blending and surface modification have been widely developed on commonly petroleum-based PS or PES membranes[1-5]. Nevertheless, the emergence of sustainable and environmentally benign PLA membranes shows its promising applications in biomedical fields[6-8] due to its unique bio-resources, carbon neutral and low cost.

Recently, PLA porous membranes with controllable structure, high water permeability and good separation performance have been developed via phase inversion process[9-11]. The hemocompatibility and anti-fouling property of PLA membranes were also investigated. In our previous work, poly(lactic acid)-block-poly(2-hydroxyethyl methacrylate) copolymer was synthesized as an additive to enhance the hydrophilicity, water permeability, antifouling and hemocompatibility of PLA membranes[12]. Dopamine was used to glue the hydrophilic substance and anticoagulant, such as zwitterionic poly(sulfobetaine methacrylate)[13] and heparin on PLA membrane surface[14]. The results showed that the anti-fouling property and hemocompatibility of PLA membranes were improved remarkably. However, the corresponding production process is either complicated or altering the property of the original membrane. Besides, the usage of dopamine will cause a brown or even dark surface, which is undesirable for the dialysis module. Therefore, a more convenient method with high efficiency and low cost is highly desirable.

Due to the excellent hydrophilicity and biocompatibility, polyethylene glycol (PEG) has been extensively used to modify polymeric membranes[15-19]. A hydration layer was restrained by PEG brushes to provide the wettability and protein resistance. However, the massive dissolution and loss of blend PEG is inevitable due to the good water solubility. Binding PEG to hydrophobic component[20, 21] and crosslinking PEG segments[22] are two main methods to inhibit the loss of PEG. Many efforts have been devoted to synthesizing PEG-containing amphiphilic copolymers, using popular routes such as free radical polymerization, ionic polymerization and copolycondensation[23-25]. Amphiphilic block copolymers, such as PLA-PEG-PLA[26, 27] were synthesized as additives to enhance the hydrophilicity and antifouling capacity of PLA membranes.

In this study, PEGDA (CH_2=CHCO(OCH_2CH_2)$_N$OCOCH=CH_2) was crosslinked on the surface of PLA membranes via a UV-induced free radical polymerization. PEGDA is a derivative with two active terminal groups, which allows the formation of self-crosslinking network[28, 29]. The reticular crosslinking PEGDA is persistently immobilized on the membrane surface and endows the membrane with improved hydrophilicity, biocompatibility/hemocompatibility and fouling resistance[22]. PLA membranes were immersed in the mixture of PEGDA, dimethylsulfoxide (DMSO) and water for micro-swelling, which allowed the deep penetration and entanglement of PEGDA with PLA segments. The entangled PEGDA was then crosslinked on the membrane surface via UV-

induced free radical polymerization. The influences of micro-swelling and crosslinking on the morphology, chemistry, permeability, hydrophilicity, protein fouling resistance and hemocompatibility were investigated respectively. Overall, the objective of our work is to provide a feasible method to prepare anti-fouling, hemocompatible PLA membranes.

Experimental section

2.1 Materials

Poly (lactic acid) (PLA, 2003D, Natural Works, US) was used to prepare membranes. Dimethylsulfoxide dehydrated (DMSO) was supplied by Sinopharm Chemical reagent Co. Polyethyleneglycoldiacrylate (PEGDA, Mn 4,000), 2-hydroxy-2-methylpropiophenone (1173) and bovine serum albumin (BSA, Mw 67,000) were purchased from Aladdin, China and used directly. Platelet-rich plasma (PRP) and platelet-poor plasma (PPP) of cow were supplied by NingBo BioChance Co., Ltd., China.

2.2 Preparation of PLA membranes

18.0 g PLA was dissolved into 82.0 g DMSO in a stirring round bottom flask at 80 °C. After the air bubbles were removed, the solution was casted onto a glass plate by a blade with thickness of 200 μm and coagulated into a water bath at 30 °C. Afterwards, the membranes were soaked into deionized water to remove the residue solvent to obtain original PLA membranes for further modification and characterization.

2.3 Surface crosslinking of PLA membranes

PLA membranes (10 cm × 10 cm) were immersed in the reactive mixture for 2 h to a certain micro-swelling degree, which is favourable for the penetration and entanglement of PEGDA with PLA chains. The content of DMSO in the mixture was set as 0/100, 10/100, 30/100 and 50/100 respectively. The content of monomer PEGDA was also set as 0, 1g, 3g, 5g, 7g respectively. The detailed composition including deionized water, DMSO, PEGDA, photoinitiator 1173 was listed in Table 1. UV-irradiation (wavelength 312 nm, irradiation distance 15 cm) was conducted for 180 s, and PEGDA was immobilized on the membrane surface through self-crosslinking.

Table.1 Composition of reactive mixture including deionized water, DMSO, PEGDA and photoinitiator 1173

Name*	m_{water} (g)	m_{DMSO} (g)	m_{PEGDA} (g)	m_{1173} (g)
M0@0	100.00	0.00	0.00	0.00
M3@0	100.00	0.00	3.00	0.04
M0@10	90.00	10.00	0.00	0.00
M3@10	90.00	10.00	3.00	0.04
M0@30	70.00	30.00	0.00	0.00
M3@30	70.00	30.00	3.00	0.04
M0@50	50.00	50.00	0.00	0.00
M3@50	50.00	50.00	3.00	0.04
M1@30	70.00	30.00	1.00	0.04
M5@30	70.00	30.00	5.00	0.04
M7@30	70.00	30.00	7.00	0.04
M10@30	70.00	30.00	10.00	0.04

*: The membrane names are Mx@y, where x and y means the content of PEGDA and DMSO in solution. For example, M3@30 means the concentrations of PEGDA and DMSO in the solution are 3% and 30%, respectively.

2.4 Characterization of PLA membranes

Surface morphologies of PLA membranes were observed by scanning electron microscope (SEM, Hitachi S-4800, Japan). The membrane roughness was measured by atomic force microscopy (AFM, Dimension 3100V, Veeco, US). The average pore size of PLA membranes was evaluated by liquid-liquid porometer (LLP-1200A, Porous Materials Inc. US), according to the procedure reported before[30]. The surface chemistry of PLA membranes was analyzed by attenuated total reflectance Fourier transform infrared spectroscopy (ATR-FTIR, Thermo-Nicolet 6700, America) and X-ray photoelectron spectroscopy (XPS, Shimadzu Axis Utltradld, Japan).

2.5 Filtration performance

The pure water flux and BSA permeability of the membranes was measured by a filtration apparatus (Saifei Company, China) with an effective membrane area of 24 cm^2. After being pre-pressured at 0.15 MPa for 30 min by deionized water, the stable flux was recorded every 5 min at 0.1 MPa, named as pure water flux (J_1). The pure water was then replaced by 1.0 g/L BSA phosphate buffer saline (PH 7.4). The BSA flux was named as J_2, and the BSA rejection ratio (R) was calculated by equation (1):

$$R(\%)=\left(1-\frac{C_{BSA}^{filtrate}}{C_{BSA}^{original}}\right)\times 100\% \quad (1)$$

Where the $C_{BSA}^{original}$ and $C_{BSA}^{filtrate}$ are BSA concentrations of the original solution and the filtrate.

In the final step, the membranes were cleaned by vibrating deionized water for 10 min, and then the recovered water flux (J_3) was evaluated.

The anti-fouling performances of the membranes were evaluated by the flux recovery ratio (FRR) and total fouling (Ft), calculated by equation (2) and (3):

$$FRR=\frac{J_3}{J_1} \quad (2)$$

$$F_t=\frac{J_1-J_2}{J_1} \quad (3)$$

2.6 Hemocompatibility

2.6.1 BSA adsorption

Bovine serum albumin (BSA) was used as the model protein to evaluate the protein adsorption of the membranes. Membrane samples with an area of 12.5 cm^2 were incubated in BSA solution (10 mL, 1.0 g/L) for 8 h. The amount of adsorbed BSA on membrane sample was calculated by comparing the

concentration of BSA solution before and after incubation, according to the Bradford method [31].

2.6.2 Activated partial thromboplastin time (APTT)

The membrane samples (1 cm × 1 cm) were incubated with 150 μl platelet-poor plasma (PPP) at 37 °C for 30 min. APTT was measured by an automated blood coagulation analyzer CA-50 (Sysmex Corp., Kobe, Japan).

2.6.3 Platelet adhesion

All membrane samples were washed with PBS buffer solution (pH 7.4). Then 100 μl platelet-rich plasma (PRP) was added onto the membrane surface and maintained at 37 °C for 1 h. After that, the samples were rinsed in PBS solution twice to remove unstable platelet and treated with 2.5 wt% glutaraldehyde for one night to fasten the adsorbed platelets. The samples were then dehydrated with 10%, 30%, 50%, 70%, 90% and 100% (v/v) ethanol/water solutions in sequence. After drying, the morphologies of adhering platelets on PLA membrane were observed by SEM.

3. Results and discussion

3.1 Membrane surface composition

The mechanism of surface crosslinking of PEGDA on PLA membrane via UV irradiation was proposed in Fig. 1. Diluted DMSO solution endowed PLA membrane with micro-swollen and flexible surface, which facilitated the entrapping of PEGDA. Subsequently, the entrapped PEGDA was able to tangle with PLA and self-crosslink on the membrane surface under UV-irradiation. Thus, a firm self-crosslinking PEGDA network was successfully immobilized on PLA membrane surface.

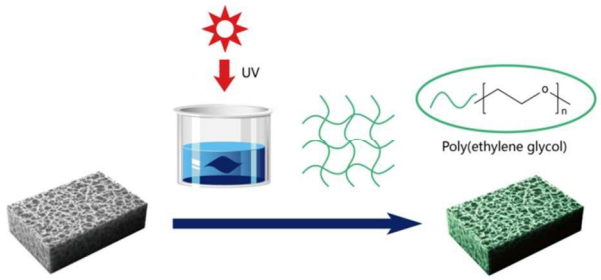

Fig.1 Mechanism of crosslinking PEGDA on PLA membrane

The surface chemistry of PLA membranes before and after surface crosslinking modification was analyzed by ATR-FTIR and XPS. As shown in Fig.2, compared with original PLA membrane (M0@0), the modified PLA membrane (M3@0) demonstrated two new absorptions at 2872 cm^{-1} and 1640 cm^{-1}, attributed to the stretch vibration of C-H and acrylate in PEGDA, respectively. To further confirm the presence of PEGDA, XPS was conducted as shown in Fig.3. In contrast to the characteristic peak 1, 2, 3 assigned to the C of PLA (M0@0), a new peak 4 appeared in the curve of the modified PLA membrane M3@0, which was attributed to the -CH_2- in PEGDA. Therefore, both ATR-FTIR and XPS confirmed that PEGDA was successfully immobilized on PLA membrane surface via UV initiated self-crosslinking.

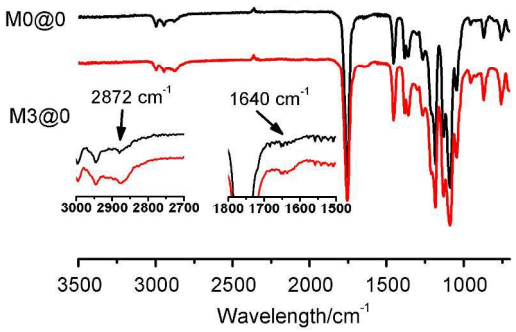

Fig.2 ATR-FTIR spectrums of PLA membranes through surface crosslinking.

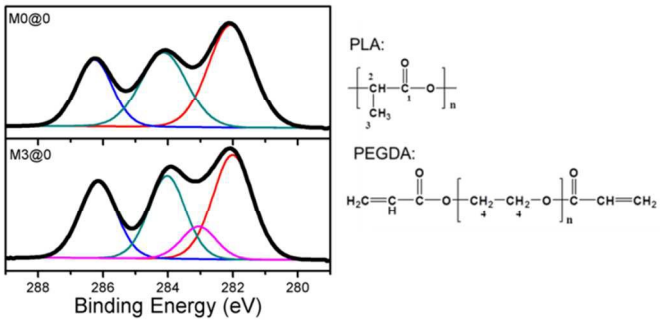

Fig.3 XPS C_{1s} region of PLA membranes through surface crosslinking.

3.2 Membrane surface morphologies

The surface morphologies of PLA membranes were investigated by SEM as shown in Fig.4. The top surface of original PLA membranes was quite porous but full of irregular pores. The solvent involved micro-swelling treatment promoted the rearrangement and assembly of irregular pores. With increasing the content of solvent in the mixture, the surface cramped pores disappeared and the whole top surface was getting denser and smoother as shown in the swollen membrane M0@10, M0@30 and M0@50. The average pore diameter (Ra) of PLA membrane (M0@0) is 45.4 nm. While, the pore size of swollen membrane is 34.4 nm, 19.6 nm and 17.2 nm for M0@10, M0@30 and M0@50 membrane, respectively. After the further crosslinking of PEGDA, the modified membrane exhibited less porous but presented more regular pores as shown in membrane M3@0, M3@10, M3@30 and M3@50. The pore size of membrane M3@50 is as small as 6.7 nm. The variation of surface morphology revealed that the micro-swelling and crosslinking could effectively tune the pore size distribution and narrow the pore size as well.

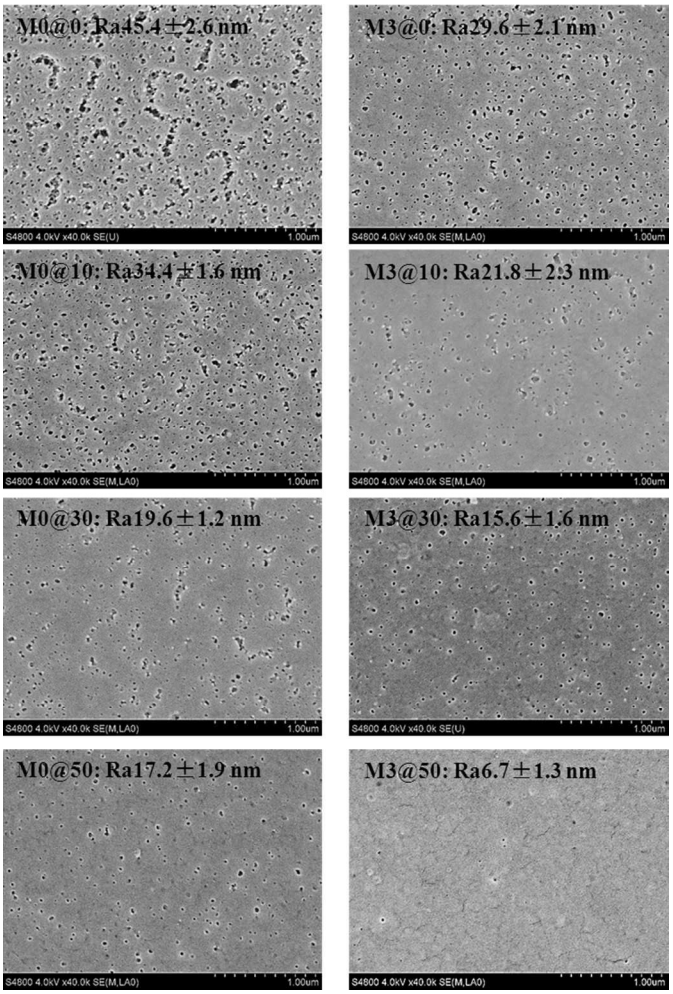

Fig.4 SEM images of the top surface of PLA membranes swollen by solvent of different DMSO content.

The micro-swelling membrane M0@30 showed appropriate pore size distribution and therefore was chose for further hydrophilic modification. The influences of PEGDA content (1 wt%, 3 wt%, 5 wt%, 7 wt% and 10 wt%) on the surface crosslinking were studied in Fig.5. It showed that the pore size decreased to some extents and the surface was getting denser with increasing the content of PEGDA. The average pore size of M1@30 membrane was 18.8 nm, while the average pore size of membrane M3@30, M5@30, M7@30 and M10@30 was decreased to 15.6 nm, 12.3 nm, 9.2 nm and 5.3 nm, respectively. PEGDA are mainly self-crosslinked under UV and entangled physically with PLA segments. Besides, PEGDA was also possibly crosslinked through the covalent bonding between the terminal double bonds and active free radicals of PLA degradation under UV irradiation. The pores size was consequently decorated and covered by the crosslinking PEGDA network. With increasing the content of PEGDA to 7 wt% and 10 wt%，a transparent, thick and sticky hydrogel was formed on the white membrane surface due to the excessive crosslinking as remarked in Fig.6.

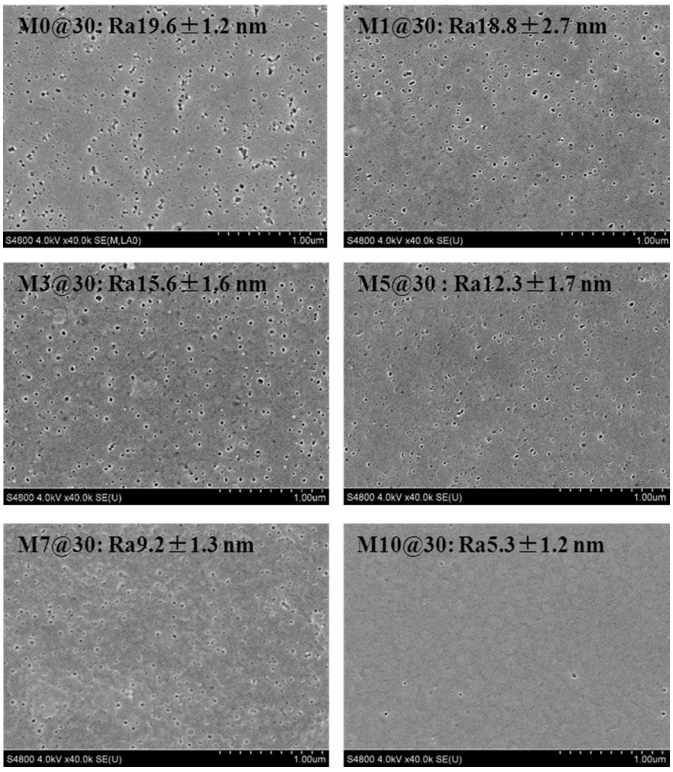

Fig.5 SEM images of the top surface of PLA membranes crosslinked with different content of PEGDA

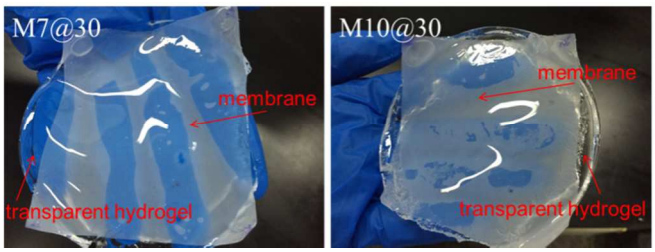

Fig.6 PLA Membrane M7@30 and M10@30 covered by transparent hydrogel

3.3 Water flux and BSA rejection

The pure water flux and BSA rejection of PLA membranes were measured. As shown in Fig.7(A), the flux and BSA rejection of original PLA membrane (M0@0) was about 316 L/m^{2}h and 67%. With increasing the content of DMSO, The flux of micro-swollen PLA membrane declined, while the BSA rejection increased，which is in accordance with the pore size variation in Fig.4. The further self-crosslinking of PEGDA on the swollen PLA membrane surface simultaneously enhanced both water flux and BSA rejection due to the better hydrophilicity and smaller pore size. For example, the water flux and BSA rejection of membrane M3@30 was increased to 283 L/m^{2}h and 90%, in contrast to 123 L/m^{2}h and 85% of membrane M0@30. The abundant water channels were constructed in the crosslinking PEGDA network, which allows water to go through freely while rejecting BSA. Hence, the influence of PEGDA crosslinking on the flux and BSA rejection was investigated. It was exhibited that the water flux increased and then declined, while the BSA rejection kept increased with PEGDA content enhanced, as shown in Fig.7(B). The membrane M3@30 demonstrated the best ultrafiltration performance with the water flux 283 L/m^{2}h, BSA rejection 90% and average pore size of 15.6 nm. The balance of

hydrophilicity and pore size variation dominated the filtration performances.

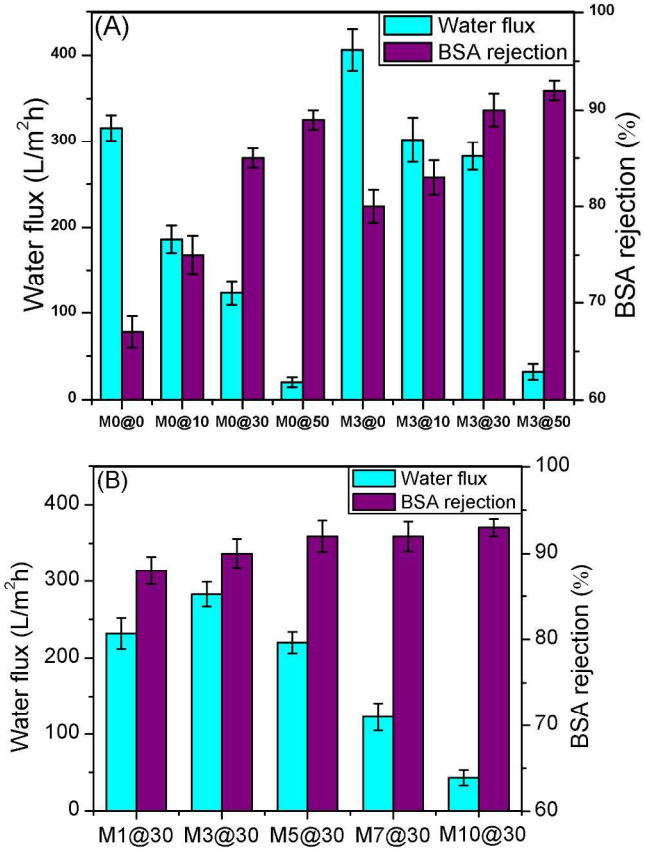

Fig.7 Water flux of PLA membranes modified in solution with different content of DMSO (A) and PEGDA (B)

3.4 Surface hydrophilicity and anti-fouling performances

Surface hydrophilicity of PLA membranes was characterized by static water contact angle (SWCA). As shown in Fig.8 (A), the original PLA membrane (M0@0) showed a SWCA of 83.2°, implying its hydrophobicity in nature. All crosslinked PLA membranes exhibited decreased SWCA and enhanced hydrophilicity. Besides, it is interesting to find that the hydrophilicity was enhanced by micro-swelling. The contact angle of membrane M3@50 was decreased to 42.3°. In order to investigate the anti-fouling properties of PLA membranes, BSA was chose as a model foulant, and water flux recovery ratio (FRR) and total fouling (F_t) was calculated to characterize the anti-fouling performance. As shown in Fig.8 (B) and (C), F_t decreased with increasing the content of DMSO in the mixture, indicating that less protein was adsorbed on the membrane surface. Moreover, the FRR of membrane M0@0 was 25.9%. After crosslinking PEGDA, the FRR reached 64.1%, 71.2% and 78.1% for M3@0, M3@10 and M3@30 respectively, indicating better anti-fouling capability.

The hydrophilicity and fouling resistance variation suggested that the micro-swelling plasticized and softened the amorphous PLA, depressed the interfacial exclusion between hydrophobic PLA surface and hydrophilic PEGDA, promoted the entanglement of PEGDA with PLA, thereafter more PEGDA network was immobilized on membrane surface. The surface chemistry was characterized by XPS to confirm this explanation as shown in Fig.9. The characteristic peaks of number 1, 2, 3 were attributed to the C of PLA and the peak of number 4 was attributed to the -CH_2- in PEGDA. The percentages of area for each peak of different membranes were listed in table.2, which obviously showed that the intensity of peak 4 increased from 5.79% to 16.42% with micro-swelling. Therefore, it was inferred that the micro-swelling promoted the crosslinking of PEGDA and resulted in enhanced hydrophilicity and anti-fouling performance.

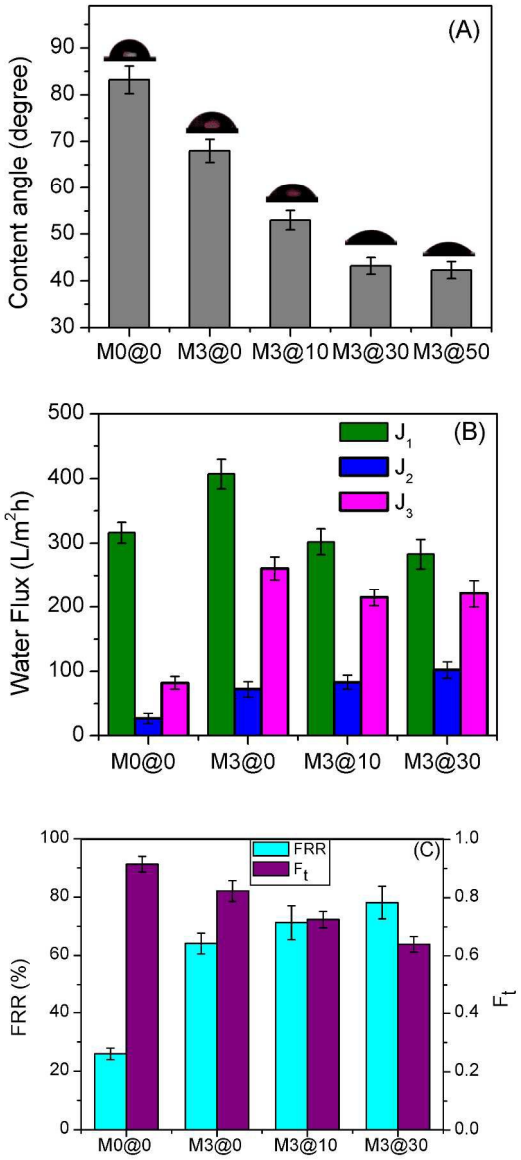

Fig.8 (A) Static water contact angles of PLA membranes by micro-swelling. (B) Pure water flux (J_1), BSA solution flux (J_2), and recovery pure water flux (J_3) of these membranes. (C) Water flux recovery ratio (FRR) and total fouling (F_t) of these membranes.

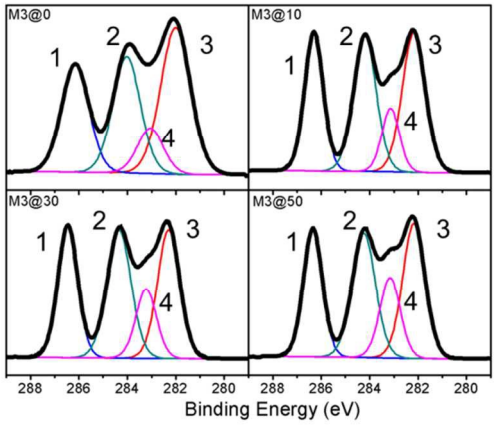

Fig.9 XPS C_{1s} region of the PLA membranes modified in solution with different weight ratio of DMSO.

Table.2 Percentages of area for each peak of PLA membranes modified in solution with different weight ratio of DMSO.

Type of membrane	Percentage of peak 1 (%)	Percentage of peak 2 (%)	Percentage of peak 3 (%)	Percentage of peak 4 (%)
M3@0	22.49	31.28	38.34	7.89
M3@10	25.83	30.60	32.29	11.29
M3@30	26.19	30.62	28.95	14.24
M3@50	24.29	28.96	30.33	16.42

Furthermore, the influence of PEGDA content on the membrane surface crosslinking was investigated, while the weight ratio of DMSO and water was set as 30:70. The decline of contact angle showed the hydrophilicity was improved remarkably as shown in Fig.10(A). Besides, as exhibited in Fig.10(B) and (C), with increasing the weight ratio of PEGDA, the FRR of modified membranes was higher and reached up to 88.4% for M10@30, meanwhile, the F_t of membranes was lowered to 0.28. As analyzed by XPS in Fig.11, more PEGDA was cross-linked on the membrane surface when the membranes were immersed in the solution with higher content of PEGDA. The percentages of area for each peak of different membranes were listed in Table.3. It showed that the intensity of peak 4 increased from 12.56% (M1@30) to 17.11% (M10@30). Therefore, the anti-fouling performances of modified membranes are significantly improved with surface crosslinking PEGylation.

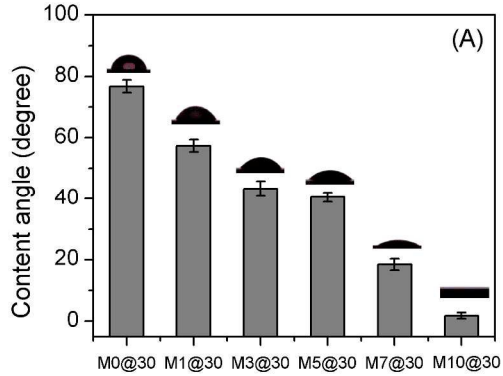

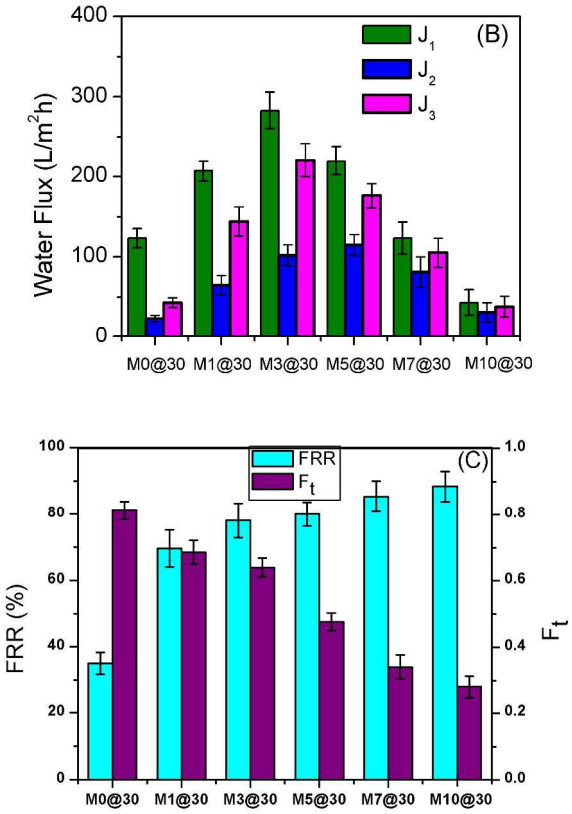

Fig.10 (A) Static water contact angles of PLA membranes by surface crosslinking with different content of PEGDA. (B) Pure water flux (J_1), BSA solution flux (J_2), and recovery pure water flux (J_3) of above membranes. (C) Water flux recovery ratio (FRR) and total fouling (F_t) of above membranes.

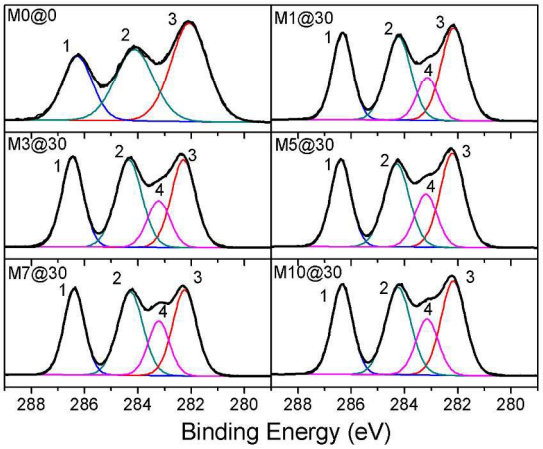

Fig.11 XPS C_{1s} region of the PLA membranes modified in solution with different weight ratio of PEGDA.

Table.3 Percentages of area for each peak of PLA membranes modified by surface crosslinking with different content of PEGDA.

Type of membrane	Percentage of peak 1 (%)	Percentage of peak 2 (%)	Percentage of peak 3 (%)	Percentage of peak 4 (%)

M1@30	24.83	29.32	33.29	12.56
M3@30	26.19	30.62	28.95	14.24
M5@30	24.10	28.33	31.37	16.20
M7@30	24.82	29.70	29.09	16.39
M10@30	24.15	28.62	30.11	17.12

3.5 Hemocompatibility

BSA adsorption, platelet adhesion and activated partial thromboplastin time (APTT) were applied to evaluate the hemocompatibility of PLA membranes after PEGylation modification.

The adsorption of BSA and APTT of the membranes was shown in Fig.12. It was clearly shown that the BSA adsorption of the modified membranes decreased and APTT increased generally. For example, BSA adsorption decreased to 35.7 μg/cm^2 and APTT increased to 78.4 s for membrane M5@30, which is almost 200% of the original PLA.

However, when the content of PEGDA reached 10%, the BSA adsorption increased and APTT decreased slightly compared to those of membrane M5@30. When the content of PEGDA was above 7%, the sticky hydrogel formed on the surface of membranes induced the contraction of membrane and affected the membrane morphology. The roughness was increased when PEGDA content was above 7%, as revealed in Fig.13, which caused more BSA adhesion and shorter APTT.

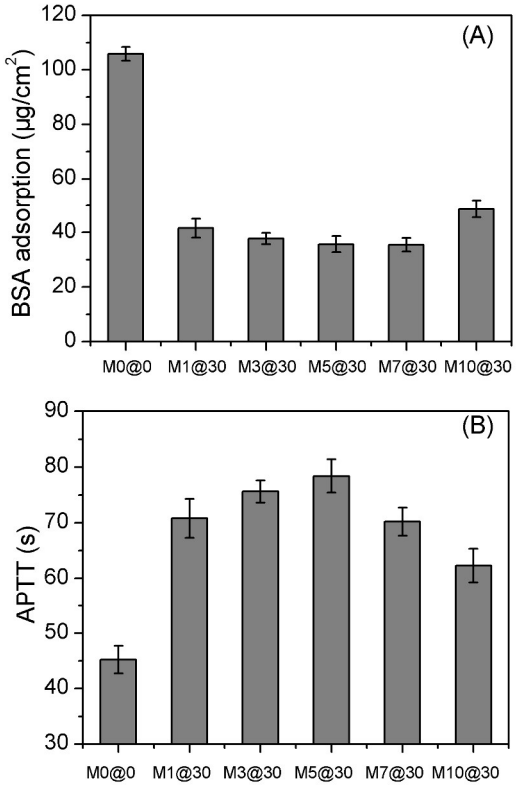

Fig.12 BSA adsorption (A) and activated partial thromboplastin time (APTT) of membranes with surface crosslinked by PEGDA of different contents.

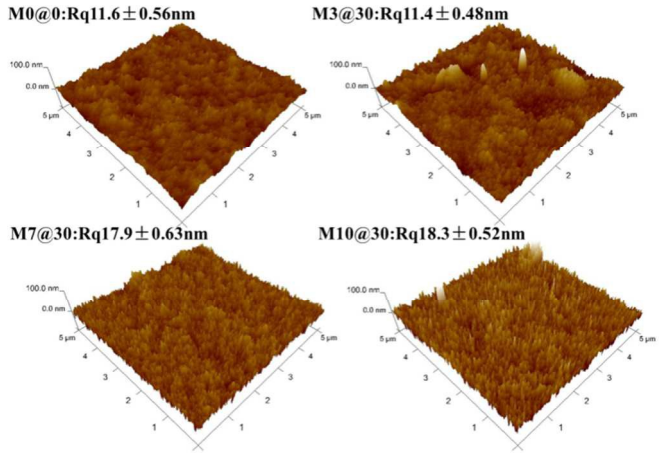

Fig.13 AFM images of PLA membranes by surface crosslinking with different content of PEGDA.

The SEM morphologies of platelet adhesion on the membranes after surface PEGylation were revealed in Fig.14. The original PLA membranes (M0@0) adsorbed platelets quite seriously, besides, the shape of platelet was outspread and distorted, indicating the activation and deformation of platelets. After surface PEGylation, fewer platelets were found on M1@30, M3@30 membrane surface. Furthermore, the formed platelets were spherical, indicating that the activation was effectively suppressed and the biocompatibility of membranes was improved. The number of the adherent platelets on the surfaces of membrane was calculated and the average value was shown in Fig.15, the number of adherent platelets on M0@0 was high, and then decreased obviously for M1@30 and M3@30. However, more platelets appeared on the membrane surface of M10@30, probably due to the excessive crosslinked hydrogel and high roughness. It matched the regularity of APTT times. Compared with the reported poly (ether sulfone) membrane[32, 33], our modified PLA membranes showed similar APTT and better static water contact angle, about 80 s and 45° respectively. Besides, the high flux and BSA rejection indicated the modified PLA membranes showed promising potential in ultrafiltration and hemodialysis.

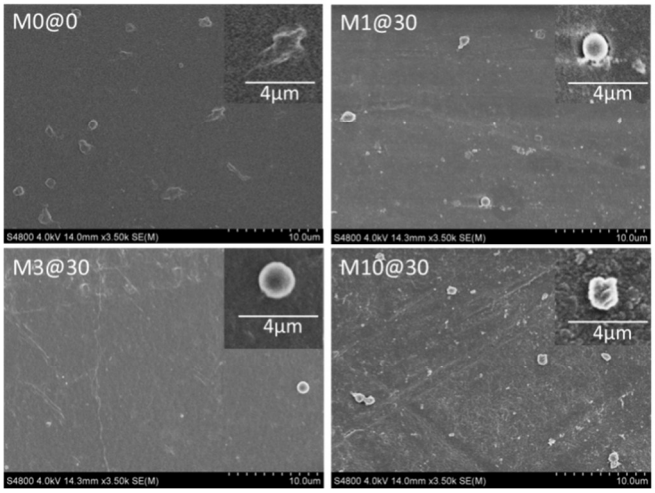

Fig.14 The typical SEM images of the adherent platelets on the surfaces of membranes by surface crosslinking with different content of PEGDA.

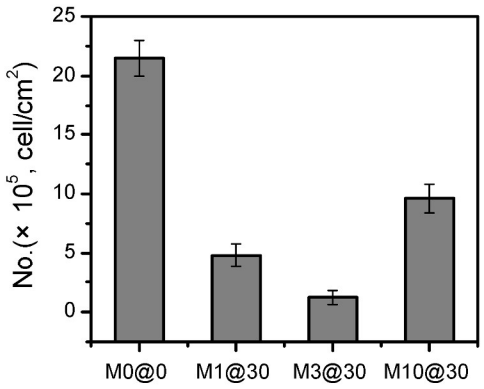

Fig.15 The number of the adherent platelets on the surfaces of membrane.

Conclusion

Surface PEGylation of PLA membrane was accomplished by micro-swelling and crosslinking of PEGDA. Both ATR-FTIR and XPS confirmed the immobilization of PEGDA on membrane surface. The content of DMSO in the mixture and the content of PEGDA have a positive effect on tuning the membrane morphology and narrowing the pore size distribution. The surface PEGylation improved the BSA rejection significantly while keeping the water flux almost unchanged for membrane M3@30. The membrane M3@30 demonstrated the best ultrafiltration performance with the water flux of 283 L/m^{2}h, BSA rejection of 90% and the average pore size of 15.6 nm. The micro-swelling promoted the crosslinking of PEGDA via plasticizing and softening the PLA membrane surface. The surface PEGylation obviously enhanced the hydrophilicity and fouling resistance. Both BSA adsorption and platelets adhesion were significantly suppressed. APTT was also extended substantially due to the surface PEGylation. The modified PLA membrane M5@30 exhibited APTT 78.4s, which is 173% of that of original one. However, the excessive crosslinking is not favourable for APTT due to the sticky hydrogel and high roughness. All results demonstrated that surface micro-swelling and crosslinking is a feasible and efficient strategy to improve the biocompatibility/hemocompatibility of PLA membrane, indicating promising application in ultrafiltration and hemodialysis membranes.

Acknowledgements

This work is supported by National Natural Science Foundation of China (51473177, 51273211).

Notes and references

Ningbo Institute of Materials Technology & Engineering, Chinese Academy of Sciences, Ningbo, 315201, P. R. China
Tel.: 86-574-86325963; E-mail: fu.liu@nimte.ac.cn

Electronic Supplementary Information (ESI) available: [details of any supplementary information available should be included here]. See DOI: 10.1039/b000000x/

1. T. Xiang, C.-D. Luo, R. Wang, Z.-Y. Han, S.-D. Sun and C.-S. Zhao, *Journal of Membrane Science*, 2015, **476**, 234-242.
2. C. Zhao, X. Liu, M. Nomizu and N. Nishi, *Biomaterials*, 2003, **24**, 3747-3755.
3. L. Li, Z. Yin, F. Li, T. Xiang, Y. Chen and C. Zhao, *Journal of Membrane Science*, 2010, **349**, 56-64.
4. L. Wang, J. Wang, X. Gao, Z. Liang, B. Zhu, L. Zhu and Y. Xu, *Polymer Chemistry*, 2014, **5**, 2836-2842.
5. L. Wang, Y. Cai, Y. Jing, B. Zhu, L. Zhu and Y. Xu, *Journal of colloid and interface science*, 2014, **422**, 38-44.
6. N. Mackiewicz, J. Nicolas, N. g. Handké, M. Noiray, J. Mougin, C. Daveu, H. R. Lakkireddy, D. Bazile and P. Couvreur, *Chemistry of Materials*, 2014, **26**, 1834-1847.
7. C. Ding, Z. Qiao, W. Jiang, H. Li, J. Wei, G. Zhou and K. Dai, *Biomaterials*, 2013, **34**, 6706-6716.
8. K. G. Battiston, J. W. Cheung, D. Jain and J. P. Santerre, *Biomaterials*, 2014, **35**, 4465-4476.
9. A. Gao, F. Liu, H. Shi and L. Xue, *Journal of Membrane Science*, 2015, **478**, 96-104.
10. A. Moriya, T. Maruyama, Y. Ohmukai, T. Sotani and H. Matsuyama, *Journal of Membrane Science*, 2009, **342**, 307-312.
11. X. Yu, F. Liu, L. Wang, Z. Xiong and Y. Wang, *RSC Advances*, 2015, **5**, 78306-78314.
12. L. Zhu, F. Liu, X. Yu and L. Xue, *ACS applied materials & interfaces*, 2015, **7**, 17748-17755.
13. L.-J. Zhu, F. Liu, X.-M. Yu, A.-L. Gao and L.-X. Xue, *Journal of Membrane Science*, 2015, **475**, 469-479.
14. A. Gao, F. Liu and L. Xue, *Journal of Membrane Science*, 2014, **452**, 390-399.
15. M. Nyström and P. Järvinen, *Journal of membrane science*, 1991, **60**, 275-296.
16. X. Zou, E. Kang and K. Neoh, *Surface and Coatings Technology*, 2002, **149**, 119-128.
17. F.-Q. Nie, Z.-K. Xu, X.-J. Huang, P. Ye and J. Wu, *Langmuir*, 2003, **19**, 9889-9895.
18. N. Meyerbröker, T. Kriesche and M. Zharnikov, *ACS applied materials & interfaces*, 2013, **5**, 2641-2649.
19. N. Meyerbröker and M. Zharnikov, *Advanced Materials*, 2014, **26**, 3328-3332.
20. W. He, H. Jiang, L. Zhang, Z. Cheng and X. Zhu, *Polymer Chemistry*, 2013, **4**, 2919-2938.
21. S. De, C. Stelzer and A. Khan, *Polymer Chemistry*, 2012, **3**, 2342-2345.
22. G. Kang, Y. Cao, H. Zhao and Q. Yuan, *Journal of Membrane Science*, 2008, **318**, 227-232.
23. H. Petersen, P. M. Fechner, D. Fischer and T. Kissel, *Macromolecules*, 2002, **35**, 6867-6874.
24. A. Asatekin, S. Kang, M. Elimelech and A. M. Mayes, *Journal of Membrane Science*, 2007, **298**, 136-146.
25. K. Knop, R. Hoogenboom, D. Fischer and U. S. Schubert, *Angewandte Chemie International Edition*, 2010, **49**, 6288-6308.
26. A. Moriya, P. Shen, Y. Ohmukai, T. Maruyama and H. Matsuyama, *Journal of Membrane Science*, 2012, **415**, 712-717.
27. P. Shen, A. Moriya, S. Rajabzadeh, T. Maruyama and H. Matsuyama, *Desalination*, 2013, **325**, 37-39.
28. H. Lin, T. Kai, B. D. Freeman, S. Kalakkunnath and D. S. Kalika, *Macromolecules*, 2005, **38**, 8381-8393.
29. H. Lin and B. D. Freeman, *Macromolecules*, 2005, **38**, 8394-8407.
30. H. Shi, F. Liu and L. Xue, *Journal of Membrane Science*, 2013, **437**, 205-215.
31. M. M. Bradford, *Analytical biochemistry*, 1976, **72**, 248-254.
32. S. Nie, M. Tang, Z. Yin, L. Wang, S. Sun and C. Zhao, *Biomaterials Science*, 2014, **2**, 98-109.
33. S. Nie, J. Xue, Y. Lu, Y. Liu, D. Wang, S. Sun, F. Ran and C. Zhao, *Colloids and Surfaces B: Biointerfaces*, 2012, **100**, 116-125.

Graphic abstract

Surface PEGylation on PLA membranes via micro-swelling and crosslinking for improved biocompatibility/hemocompatibility

Xuemin Yu, Zhu Xiong, Jinglong Li, Ziyang Wu, Yunze Wang, Fu Liu*

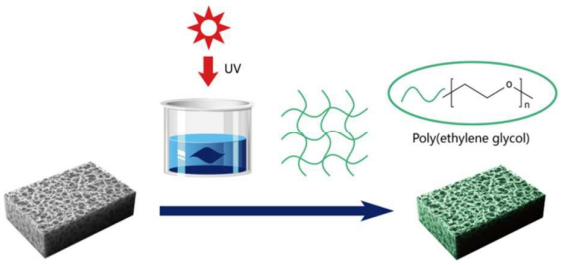

A feasible and efficient strategy was developed to enable the persistent PEGylation on PLA membrane surface via micro-swelling and subsequent UV-initiated crosslinking of poly (ethylene glycol) diacrylate.